
Assessment of Simplified Methods to Measure ^{18}F -FLT Uptake Changes in EGFR-Mutated Non–Small Cell Lung Cancer Patients Undergoing EGFR Tyrosine Kinase Inhibitor Treatment

Virginie Frings¹, Maqsood Yaqub¹, Lieke L. Hoyng¹, Sandeep S.V. Golla¹, Albert D. Windhorst¹, Robert C. Schuit¹, Adriaan A. Lammertsma¹, Otto S. Hoekstra¹, Egbert F. Smit², and Ronald Boellaard¹, for the QuIC-ConCePT Consortium

¹Department of Radiology and Nuclear Medicine, VU University Medical Center, Amsterdam, The Netherlands; and ²Department of Pulmonology, VU University Medical Center, Amsterdam, The Netherlands

3'-deoxy-3'- ^{18}F -fluorothymidine (^{18}F -FLT) PET/CT provides a noninvasive assessment of proliferation and, as such, could be a valuable imaging biomarker in oncology. The aim of the present study was to assess the validity of simplified quantitative parameters of ^{18}F -FLT uptake in non–small cell lung cancer (NSCLC) patients before and after the start of treatment with a tyrosine kinase inhibitor (TKI). **Methods:** Ten patients with metastatic NSCLC harboring an activating epidermal growth factor receptor mutation were included in this prospective observational study. Patients underwent ^{15}O - H_2O and ^{18}F -FLT PET/CT scanning on 3 separate occasions: within 7 d before treatment, and 7 and 28 d after the first therapeutic dose of a TKI (gefitinib or erlotinib). Dynamic scans were acquired and venous blood samples were collected during the ^{18}F -FLT scan to measure parent fraction and plasma and whole-blood radioactivity concentrations. Simplified measures (standardized uptake value [SUV] and tumor-to-blood ratio [TBR]) were correlated with fully quantitative measures derived from kinetic modeling. **Results:** Twenty-nine of thirty ^{18}F -FLT PET/CT scans were evaluable. According to the Akaike criterion, a reversible 2-tissue model with 4 rate constants and blood volume parameter was preferred in 84% of cases. Relative therapy-induced changes in SUV and TBR correlated with those derived from kinetic analyses ($r^2 = 0.83$ – 0.97 , $P < 0.001$, slope = 0.72 – 1.12). ^{18}F -FLT uptake significantly decreased at 7 and 28 d after the start of treatment compared with baseline ($P < 0.01$). Changes in ^{18}F -FLT uptake were not correlated with changes in perfusion, as measured using ^{15}O - H_2O . **Conclusion:** SUV and TBR could both be used as surrogate simplified measures to assess changes in ^{18}F -FLT uptake in NSCLC patients treated with a TKI, at the cost of a small underestimation in uptake changes or the need for a blood sample and metabolite measurement, respectively.

Key Words: ^{18}F -FLT; PET; NSCLC; pharmacokinetic modeling; imaging biomarker

J Nucl Med 2014; 55:1417–1423

DOI: 10.2967/jnumed.114.140913

Lung cancer is the leading cause of cancer-related death worldwide, and 85% of all lung cancers are non–small cell lung cancer (NSCLC) (1). Moreover, most patients present at an advanced stage, when treatment options are limited (stages III and IV, based on the seventh edition of the TNM staging system for lung cancer (2)). Novel treatments with targeted drugs based on, among others, molecular alterations in the epidermal growth factor receptor (EGFR) have been developed for stage IV NSCLC (3). EGFR is a transmembrane receptor that is involved in cellular processes such as proliferation, angiogenesis, invasion, and resistance to apoptosis. Activating mutations in the EGFR domain result in continuous downstream effects. The intracellular tyrosine kinase part of EGFR can be inhibited reversibly by the EGFR tyrosine kinase inhibitors (TKI) gefitinib and erlotinib. Both drugs have shown efficacy in tumors harboring an activating mutation in the EGFR gene but limited efficacy in EGFR wild type (4–6). Compared with cytotoxic treatment, TKI toxicity profiles are mild and treatment results in a benefit with respect to progression-free survival. Consequently, in this subgroup of patients with an activating EGFR mutation, quality of life is improved with TKI treatment compared with cytotoxic chemotherapy (7).

To evaluate treatment response in patients, an objective non-invasive (imaging) biomarker that can be used early after the start of treatment would be useful, as it would provide a means to identify ineffective treatment at an early stage. Discontinuation of such treatment can prevent unnecessary toxicities and costs. Moreover, an imaging biomarker could provide an early readout of treatment efficacy in drug development (e.g., phase 2 and 3 trials) (8). PET/CT using 3'-deoxy-3'- ^{18}F -fluorothymidine (^{18}F -FLT) may be a good candidate, as ^{18}F -FLT is a proliferation marker and uptake of ^{18}F -FLT correlates with immunohistochemistry for proliferation in lung, brain, and breast cancer (9). In addition, changes in maximum standardized uptake values (SUVs) 7 d after the start of treatment with erlotinib correlated with response measured on CT 6 wk after the start of treatment in NSCLC patients (10). ^{18}F -FLT follows the salvage pathway of endogenous thymidine in the cell but is not incorporated into DNA (11). Published data on response evaluation using ^{18}F -FLT PET, however, are contradictory (12–14), and it is not clear to what extent this heterogeneity is related to different pharmacokinetic

Received Apr. 1, 2014; revision accepted Jun. 3, 2014.

For correspondence or reprints contact: Ronald Boellaard, Department of Radiology and Nuclear Medicine, VU University Medical Center (VUmc), P.O. Box 7057, 1007 MB Amsterdam, The Netherlands.

E-mail: r.boellaard@vumc.nl

Published online Jun. 26, 2014.

COPYRIGHT © 2014 by the Society of Nuclear Medicine and Molecular Imaging, Inc.

characteristics, biologic changes, image resolutions, or PET quantification methods. The reference method for quantification of PET studies is full kinetic modeling, which requires arterial blood sampling and dynamic scanning (15). This procedure is not suited for daily clinical practice in which whole-body acquisitions are needed, and it limits the number of centers that can take part in multicenter studies. Therefore, accurate simplified protocols and analytic methods are needed. These methods should be validated against full kinetic modeling both before and after the start of treatment, as tumor blood flow, fractional blood volume, or plasma clearance of ^{18}F -FLT may change because of treatment. Treatment-induced changes in kinetics are accounted for in kinetic modeling but not in simplified measures such as SUV or tumor-to-blood ratios (TBRs) (16), and these simplified measures should therefore be validated. The aim of this project was to perform such a technical validation study and to facilitate future biologic validation studies.

This prospective clinical study investigated whether simplified quantitative methods can be used as alternative measures to evaluate changes in ^{18}F -FLT uptake in NSCLC patients after the start of treatment with TKIs.

MATERIALS AND METHODS

Patients

Patients with stage IV NSCLC and activating EGFR mutations were recruited at 6 medical centers in The Netherlands. The institutional review board of the VU University Medical Center approved this study, and all subjects gave written informed consent. The study was included in the Dutch trial register (trialregister.nl, identification number NTR3557). Patients were scheduled for 3 dynamic ^{18}F -FLT PET/CT scans: before treatment, and 7 and 28 d after the first therapeutic dose of an EGFR TKI. Seven days was chosen as the first time point because erlotinib and gefitinib reach a steady state on day 7. The treating pulmonary physician chose the type of treatment (250 mg of gefitinib orally once a day or 150 mg of erlotinib orally once a day). All scanning was performed at the VU University Medical Center.

PET Imaging

PET scans were obtained using a Gemini TF-64 PET/CT scanner (Philips (17)) with an axial field of view of 18 cm. The scan field was determined by a nuclear physician such that the lung tumor was positioned centrally in the field of view based on a diagnostic CT scan of the thorax. Patients had been fasting for 4 h before the start of the scan to avoid possible food-induced thymidine changes. Tracer was injected and blood sampled through a venous cannula in the forearm. A 370-MBq bolus of ^{15}O - H_2O in 5 mL of saline was injected at a rate of $0.8 \text{ mL}\cdot\text{s}^{-1}$, followed by a 35-mL saline flush at $2.0 \text{ mL}\cdot\text{s}^{-1}$. At the start of the ^{15}O - H_2O injection, a dynamic emission scan was started with a total duration of 10 min, binned into 26 frames of the following lengths: 1×10 , 8×5 , 4×10 , 2×15 , 3×20 , 2×30 , and 6×60 s. Next, a low-dose CT scan with 120 kV and 50 mAs was performed to correct the former emission scan for attenuation. At least 15 min after injection of ^{15}O - H_2O to allow for decay of ^{15}O , an ^{18}F -FLT scan was obtained. This dynamic emission scan was started at the time of a bolus injection of 370 MBq of ^{18}F -FLT in 5 mL of saline (18) at a rate of $0.8 \text{ mL}\cdot\text{s}^{-1}$ followed by a 35-mL flush of saline at $2.0 \text{ mL}\cdot\text{s}^{-1}$. Immediately after injection, the rest of the activity in the syringe was measured to calculate the net injected ^{18}F -FLT dose. The ^{18}F -FLT scan was binned into 36 frames (1×10 , 8×5 , 4×10 , 3×20 , 5×30 , 5×60 , 4×150 , 4×300 and 2×600 s) with a total duration of 60 min. Afterward, a second low-dose CT scan was acquired to correct the

^{18}F -FLT scan for attenuation. All dynamic scan data were corrected for dead time, decay, scatter, and randoms and were reconstructed using the 3-dimensional row-action maximum likelihood algorithm, resulting in a transaxial spatial resolution of approximately 5 mm in full width at half maximum in the center of the field of view (17).

Venous blood samples were drawn during the dynamic ^{18}F -FLT PET scan at 5, 10, 20, 30, 40, and 60 min after injection. Three to five milliliters of blood were drawn before each sample, followed by drawing of a 7-mL sample and then flushing with 2.5 mL of saline. Whole-blood activity concentration, plasma activity concentration, and parent fraction of ^{18}F -FLT were measured for all samples (19).

PET Data Analysis

The outer 5 planes (~ 2 cm) of the field of view were not used for quantification. Tumors were delineated on an averaged image of the last 3 frames of the ^{18}F -FLT scan using a 50% threshold of SUV_{peak} corrected for local contrast as described previously (20,21). In addition, healthy lung volumes of interest (VOIs) were drawn centrally in the contralateral lung using a cylindrical VOI with a diameter of 1.2 cm and an axial length of 2.0 cm. A bone marrow VOI of 1.2-cm diameter and 2.4-cm axial length was drawn over a corpus vertebrae. Time-activity curves were generated by projecting VOIs onto all frames of the dynamic ^{15}O - H_2O and ^{18}F -FLT scans.

An image-derived input function was extracted from the ascending aorta with 2×2 voxels in 5 planes of the early frames (frames 4–6) of both ^{15}O - H_2O and ^{18}F -FLT scans, and corresponding time-activity curves were generated. Tails of the ^{18}F -FLT image-derived input function time-activity curves (interval, 500–3,600 s) were calibrated with measured radioactivity concentrations in the venous blood samples, and the entire image-derived input function time-activity curve was rescaled with this calibration factor. In addition, image-derived input functions were corrected for both plasma-to-blood ratios and metabolites to obtain calibrated parent ^{18}F -FLT plasma input functions (11).

Outcome measures of full kinetic modeling and simplified approaches were obtained using an in-house-developed software tool in MATLAB (version 7.10; The MathWorks Inc.). ^{15}O - H_2O data were analyzed using the standard single-tissue reversible plasma input model with additional blood volume parameter (22). For ^{18}F -FLT, the compartmental model underlying the biology of ^{18}F -FLT uptake has been described previously (11). Reversible and irreversible 2-tissue plasma input models were investigated for ^{18}F -FLT uptake with blood volume parameter. Individual data points of time-activity curves were weighted on the basis of frame length and whole-scanner true counts per frame (23). These weighting factors were included in the figure of merit (cost function) during curve fitting. Dual-input models for both reversible and irreversible models with blood volume parameter were evaluated to assess the effects of possible cellular uptake of labeled metabolites (24). Net influx rate (K_i) and volume of distribution (V_T) were derived from kinetic rate constants:

$$K_i = \frac{K_1 k_3}{(k_2 + k_3)} \quad \text{Eq. 1}$$

$$V_T = \frac{K_1}{k_2} \left(1 + \frac{k_3}{k_4} \right) \quad \text{Eq. 2}$$

In addition, nondisplaceable binding potential (BP_{ND}) was calculated for the reversible 2-tissue model:

$$\text{BP}_{\text{ND}} = \frac{k_3}{k_4} \quad \text{Eq. 3}$$

Simplified measures, SUV and TBR, were calculated for 2 time intervals; 40–60 min and 50–60 min:

$$\text{SUV} = \frac{\text{activity concentration VOI (kBq/mL)}}{{}^{18}\text{F-FLT dose (MBq)/normalization factor}} \quad \text{Eq. 4}$$

$$\text{TBR} = \frac{\text{activity concentration tumor (kBq/mL)}}{\text{activity concentration blood (kBq/mL)}} \quad \text{Eq. 5}$$

Normalization factors for SUV were body weight, lean body mass, and body surface area (25). For TBR, whole blood and parent plasma were used as the denominator. In addition, SUV and TBR were calculated per time frame to generate SUV and TBR curves over time.

Relative differences at 7 and 28 d after the start of treatment compared with baseline were calculated for all parameters:

$$\% \text{ difference} = \frac{\text{response} - \text{baseline}}{\text{baseline}} \times 100 \quad \text{Eq. 6}$$

Statistical Analysis

Data were tested for normality by evaluating histograms of all parameters. Mean and SD were used when the distribution was normal, and median and interquartile range (IQR) were used otherwise. The optimal pharmacokinetic model was selected on the basis of the Akaike criterion (26). Statistical analysis comprised linear regression to assess the correlation between simplified and full kinetic outcome measures. r^2 , slope, and intercept of linear regressions were derived, together with 95% confidence interval. Friedman and Wilcoxon signed-rank test were used to test for statistical differences between pre- and posttreatment scans. P values of less than 0.05 were considered significant. Statistical analyses were performed using SPSS Statistics 20 (IBM Corp.).

RESULTS

Between September 2012 and December 2013, 10 patients were included (demographics and EGFR mutation types are presented in Table 1). Baseline scans were obtained within a median of 1 d (range, 0–3 d) before the start of treatment with the exception of a single patient whose baseline scan was obtained 26 d before the start of treatment with gefitinib. This patient started erlotinib treatment after the baseline scan but stopped 5 d later because of

TABLE 1
Patient Demographics

Parameter	Data
Sex (<i>n</i>)	
Male	4
Female	6
Age (y)	
Median	64
Range	52–75
Smoking (<i>n</i>)	
Current	3
History of smoking	4
Never	3
EGFR mutation (<i>n</i>)	
Exon 18 G719X	2
Exon 19 del E746-A750	2
Exon 21 L585R	6
Treatment (<i>n</i>)	
Gefitinib	7
Erlotinib	3

gastrointestinal toxicity. Three weeks later, when symptoms had abated, gefitinib treatment was initiated and follow-up ${}^{18}\text{F-FLT}$ scans were obtained after the start of treatment with gefitinib without performing a new baseline scan (as the patient had already been pretreated with erlotinib). Follow-up scans were obtained within a median of 7 d (IQR, 6–9) and 28 d (IQR, 27–29) after the start of treatment. Body weight of patients was not significantly different between scans: 67 kg (IQR, 67–89), 68 kg (IQR, 66–89), and 67 kg (IQR, 64–89) at baseline, 7 d, and 28 d after the start of treatment, respectively (Friedman test, $P = 0.88$).

All patients completed the 3 study visits. One ${}^{18}\text{F-FLT}$ scan was not evaluable because of a scanner failure. Four ${}^{15}\text{O-H}_2\text{O}$ scans were not obtained because of technical or logistic problems. The median net injected ${}^{18}\text{F-FLT}$ doses were 383 MBq (IQR, 352–394), 376 MBq (IQR, 364–390), and 376 MBq (IQR, 365–385) for scans 1, 2, and 3, respectively (Friedman test, $P = 0.50$). Injected ${}^{15}\text{O-H}_2\text{O}$ was 370 MBq for every scan. Median parent fractions of ${}^{18}\text{F-FLT}$ at 60 min after injection were 76% (IQR, 73–84), 79% (IQR, 74–82), and 81% (IQR, 76–82) for scans 1, 2, and 3, respectively (Friedman test, $P = 0.90$). Median plasma-to-blood ratios at 60 min after injection were 1.19 (IQR, 1.13–1.27), 1.19 (IQR, 1.15–1.24), and 1.19 (IQR, 1.15–1.23) for scans 1, 2, and 3, respectively (Friedman test, $P = 0.64$). The median image-derived input function calibration factor was 0.86 (IQR, 0.80–0.94).

Twenty-four ${}^{18}\text{F-FLT}$ -avid lesions were detected at baseline, with 22 and 17 lesions evaluable (visually detected above background) at 7 and 28 d, respectively, after the start of treatment (Fig. 1). Overall, based on the Akaike criterion, a 2-tissue reversible model was preferred over a 2-tissue irreversible model in 84% (88% at baseline and 82% and 82% at 7 and 28 d, respectively, after the start of treatment; Friedman test, $P = 0.14$). Dual-input pharmacokinetic modeling did not improve kinetic analyses according to the Akaike criterion. No differences in modeling of ${}^{18}\text{F-FLT}$ kinetics between patients treated with erlotinib and patients treated with gefitinib were observed, and therefore data were pooled. The results of full kinetic modeling, and SUV and TBR analyses per scan, are shown in Table 2. V_T decreased significantly relative to baseline at both 7 d and 28 d after the start of treatment (Friedman test, $P < 0.001$). Within the evaluable lesions, no significant difference between 7 and 28 d after the start of treatment was observed (Wilcoxon signed-rank test, $P = 0.46$). SUV and TBR showed the same absolute trend as V_T . Relative changes in SUV and TBR correlated strongly with relative changes in V_T , with an r^2 of 0.83–0.97 ($P < 0.001$) and a slope of 0.72–1.12 (Fig. 2; Table 3). The intercept ranged from –5% to 12%, which was not significantly different from zero, except for TBR whole blood, which showed a positive bias of 7%–12% (Table 3). SUV reached equilibrium at 30 min after injection, whereas TBR was still increasing at 60 min after injection (Fig. 3).

${}^{18}\text{F-FLT}$ kinetics in bone marrow and normal lung were best fitted using a 2-tissue irreversible model with blood volume parameter in 56%, 90%, and 80% (bone marrow) and in 78%, 80%, and 70% (lung) for scans 1, 2, and 3, respectively (Friedman test, $P = 0.10$ and 0.72 for bone marrow and lung, respectively). ${}^{18}\text{F-FLT}$ influx in bone marrow and lung, obtained from K_i of the 2-tissue irreversible model, was not significantly different from baseline at 7 or 28 d after the start of treatment (Friedman test, $P = 0.24$ and 0.46 for bone marrow and lung, respectively).

Tumor perfusion did not significantly change after the start of treatment, with a median K_1 of ${}^{15}\text{O-H}_2\text{O}$ of 0.41 (IQR, 0.31–0.61),

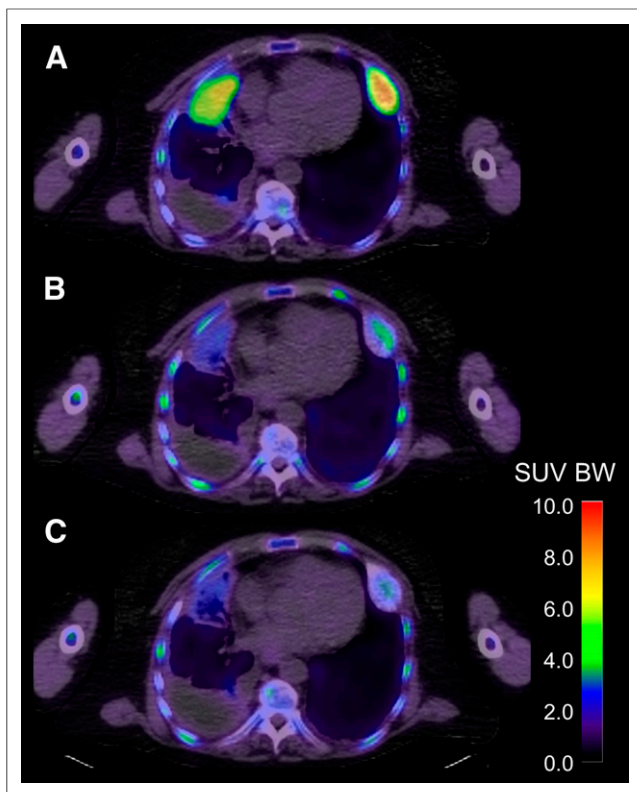


FIGURE 1. Fused ^{18}F -FLT PET/CT image of patient with stage IV NSCLC with primary tumor in right lung and contralateral bone metastasis, at baseline (A) and 7 d (B) and 26 d (C) after start of treatment with erlotinib.

0.35 (IQR, 0.25–0.59), and 0.39 (IQR, 0.29–0.77) $\text{mL}\cdot\text{cm}^{-3}\cdot\text{min}^{-1}$ for scans 1, 2, and 3, respectively (Friedman test, $P = 0.29$). Relative changes in tumor perfusion did not correlate with relative changes in ^{18}F -FLT uptake, with an r^2 of 0.05 and 0.06 at 7 and

28 d, respectively after the start of treatment ($P = 0.38$ and 0.42 ; Fig. 4).

DISCUSSION

This study investigated the correlation of relative changes in simplified and full kinetic ^{18}F -FLT measures in NSCLC patients after the start of TKI treatment to assess whether simplified measures can be used as surrogate markers of treatment response. A 2-tissue reversible model with blood volume parameter was the preferred model for tumor ^{18}F -FLT kinetics. Relative changes in SUV and TBR correlated well with relative changes in V_T ($r^2 = 0.83$ – 0.97), and therefore, these simplified measures can be used as alternative parameters to evaluate changes in ^{18}F -FLT uptake due to TKI treatment.

Parent fractions and plasma-to-blood ratios were not significantly different between baseline and after the start of treatment, suggesting that the plasma kinetics of ^{18}F -FLT are stable after the start of treatment with TKI, without inter- and intrasubject variability. Therefore, a population-based input function may be a valid alternative for kinetic analysis of response evaluation studies on patients who are treated with a TKI; however, this requires further evaluation in a larger patient group (27).

^{18}F -FLT uptake showed reversible kinetics in most lesions. Although preference for the reversible model decreased after the start of treatment, this trend was not statistically significant. An extended scan duration might provide better fits and more robust estimates of k_4 with a sustainable preference for a reversible model after the start of treatment (28). In addition to single-input-function models, dual-input-function models were investigated, to assess whether influx and efflux of metabolites play a role. However, these models did not provide better fits, and therefore results from the 2-tissue reversible model with blood volume parameter were used. From this model, the macroparameter V_T represents the most robust result and was used as a reference to assess simplified uptake measures. V_T decreased significantly after the start of treatment but was not significantly different

TABLE 2
 ^{18}F -FLT Uptake at Baseline and 7 and 28 Days After Start of Treatment

Parameter	Baseline	7 d after start of treatment	28 d after start of treatment	Friedman test P
Pharmacokinetic model				
K_1	0.294 (0.242–0.389)	0.255 (0.190–0.312)	0.260 (0.193–0.424)	0.11
k_3	0.129 (0.080–0.175)	0.083 (0.069–0.123)	0.088 (0.073–0.135)	0.05
BP_{ND}	5.66 (3.27–8.21)	3.12 (2.45–5.35)	3.64 (2.61–6.06)	0.02
V_B	0.066 (0.050–0.128)	0.082 (0.054–0.170)	0.101 (0.065–0.171)	0.001
V_T	4.53 (3.12–5.52)	3.41 (1.68–3.81)	2.99 (2.60–3.79)	<0.001
K_i	0.063 (0.051–0.082)	0.050 (0.031–0.058)	0.048 (0.040–0.063)	0.005
Simplified models				
TBR PP 40–60 min	5.0 (3.3–5.8)	3.4 (1.8–4.6)	3.5 (3.0–4.1)	0.003
TBR PP 50–60 min	5.3 (3.3–5.8)	3.5 (1.9–4.9)	3.8 (3.2–4.4)	0.001
TBR WB 40–60 min	4.3 (3.3–5.4)	3.3 (2.0–4.4)	3.4 (2.9–3.9)	0.001
TBR WB 50–60 min	4.5 (3.3–5.8)	3.5 (2.2–4.6)	3.6 (3.1–4.1)	0.001
SUV LBM 40–60 min	2.5 (2.0–3.3)	1.9 (1.2–2.5)	1.9 (1.6–2.2)	<0.001
SUV LBM 50–60 min	2.4 (2.0–3.2)	1.9 (1.2–2.5)	1.9 (1.6–2.2)	<0.001

BP_{ND} = nondisplaceable binding potential; V_B = blood volume fraction; PP = parent plasma; WB = whole blood; LBM = lean body mass.

Data are median followed by interquartile range in parentheses.

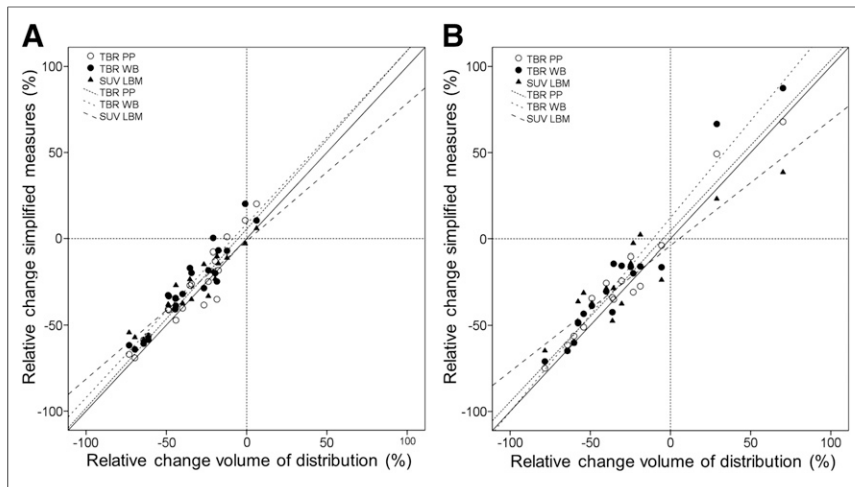


FIGURE 2. Correlation of percentage change in SUV and TBR for time interval of 50–60 min and V_T derived using 2-tissue reversible model with blood volume parameter at 7 d (A) and 28 d (B) after start of treatment. Solid line represents line of identity. LBM = lean body mass; PP = parent plasma; WB = whole blood.

between 7 and 28 d after the start of treatment (Table 2). Microparameter K_1 , which represents ^{18}F -FLT influx, did not change after the start of treatment ($P = 0.11$), suggesting that expression of nucleoside transporters to the cell membrane are not up- or downregulated after the start of treatment, as has been described in mice (29). In addition, microparameter k_3 decreased after the start of treatment ($P = 0.05$), indicating decreased thymidine kinase activity and thereby a decreased proliferation rate. Therefore, measured changes in ^{18}F -FLT uptake could be attributed to changes in phosphorylation rate (k_3) instead of cell membrane transport (K_1).

Conceptually, TBR is a simplified model for reversible kinetics and SUV for irreversible models. However, changes in both parameters strongly correlated with changes in V_T ($r^2 = 0.83$ – 0.97) and could be used to evaluate ^{18}F -FLT uptake responses. Relative differences in TBR whole blood had a significant but small positive bias, which might be caused by small differences in parent fraction per scan. Consequently, this may explain why differences in TBR parent plasma at 50–60 min after injection had a high correlation with differences in V_T (0.89 and 0.95 after 7 and 28 d, respectively), a slope that was close to the line of identity (1.04 and 0.99), and no bias (intercept not significantly different

from zero). Therefore, this parameter appears to be a sensitive measure for detecting relative changes. Unfortunately, however, TBR parent plasma was not stable over time, and differences in acquisition time could affect outcome (higher TBR parent plasma for longer uptake time intervals). In addition, both a blood VOI and a blood sample are needed to measure blood activity concentration, parent fraction, and plasma-to-blood ratio, limiting its feasibility in multicenter studies. Alternatively, SUV showed a plateau beyond 30 min after injection, and therefore measurements will be less dependent on uptake interval as long as the acquisition is performed somewhere between 30 and 60 min after injection, as reported previously (30). On the other hand, SUV underestimated relative therapy-induced changes with slopes significantly less than 1, as is in line with previous results in locally advanced

breast cancer (16). Therefore, SUV may be preferred in multicenter ^{18}F -FLT PET studies based on feasibility, but one should be aware of possible underestimation of response assessment (18%–28%) in patients treated with a TKI.

SUV normalization can be performed using body weight, lean body mass, or body surface area. For ^{18}F -FLT, lean body mass might be the best normalization factor, as ^{18}F -FLT has no specific uptake in fat or muscle. This is in agreement with the recommendation to use SUV lean body mass for response evaluation in ^{18}F -FDG PET studies (31). In the present study, body weight was not significantly different between successive scans, and consequently, SUV body weight, lean body mass, and body surface area performed similarly and no definitive decision can be made with respect to the optimal SUV normalization.

Relative changes in tumor perfusion, measured using K_1 of ^{15}O - H_2O , did not correlate with relative changes in ^{18}F -FLT uptake after the start of treatment. This finding indicates that ^{18}F -FLT uptake is independent of perfusion and that changes in ^{18}F -FLT uptake are not caused by perfusion changes.

The treatment regimen with either gefitinib or erlotinib was determined by the treating physician. Both drugs are reversible TKI with a similar mechanism of action (32,33). In the present

TABLE 3
Correlation of Relative Changes in Simplified Measures vs. V_T

Parameter	7 d after start of treatment			28 d after start of treatment		
	r^2	Slope	Intercept	r^2	Slope	Intercept
TBR PP 40–60 min	0.90	0.99 (0.83–1.14)	4 (–2–11)	0.96	0.88 (0.77–0.98)	0 (–5–5)
TBR PP 50–60 min	0.89	1.04 (0.86–1.21)	6 (–2–13)	0.95	0.99 (0.87–1.11)	5 (–1–10)
TBR WB 40–60 min	0.92	0.96 (0.83–1.10)	7 (2–13)	0.97	0.99 (0.89–1.09)	7 (2–11)
TBR WB 50–60 min	0.90	1.01 (0.84–1.17)	9 (2–15)	0.94	1.12 (0.96–1.29)	12 (5–20)
SUV LBM 40–60 min	0.90	0.78 (0.66–0.91)	–2 (–7–3)	0.83	0.72 (0.53–0.90)	–4 (–13–4)
SUV LBM 50–60 min	0.91	0.80 (0.68–0.92)	–1 (–6–4)	0.83	0.73 (0.54–0.92)	–4 (–13–5)

PP = parent plasma; WB = whole blood; LBM = lean body mass.
Data in parentheses are 95% confidence intervals.

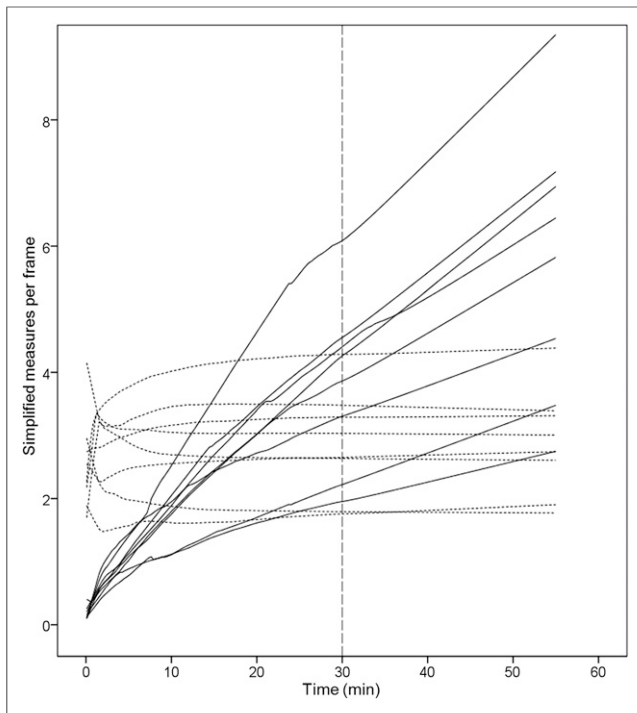


FIGURE 3. SUV lean body mass and TBR parent plasma as function of time at baseline for all patients, showing equilibrium of SUV lean body mass being reached at 30 min, whereas TBR parent plasma still increases at 60 min. Solid lines represent TBR parent plasma, and dashed lines represent SUV lean body mass.

study, data were pooled, as no differences in ^{18}F -FLT kinetics were observed between the 2 treatment regimens.

Our study described the technical validation of simplified ^{18}F -FLT uptake measures in NSCLC patients treated with TKI. Biologic validation studies, in which relative changes in simplified measures of ^{18}F -FLT uptake need to be correlated with pathology or clinical outcome, should be performed to determine the predictive value. Once this is confirmed, ^{18}F -FLT PET could qualify as a predictive biomarker of response to TKI in NSCLC. Furthermore, it is tempting to extrapolate the present positive findings of the use of simplified measures to quantify ^{18}F -FLT uptake to other tumor and treatment types. This should, however, be validated in each case separately, as systemic therapy may alter the correlation between simplified and fully quantitative measures (34).

CONCLUSION

In NSCLC patients treated with a TKI, relative changes in SUV and TBR correlated with those in V_T of ^{18}F -FLT. SUV lean body mass measured 30–60 min after injection or TBR parent plasma at 50–60 min after injection could be used for future response assessment studies in NSCLC patients with an activating EGFR mutation treated with a TKI, at the cost of a small underestimation in uptake changes or the need for a blood sample and metabolite measurement, respectively.

DISCLOSURE

The costs of publication of this article were defrayed in part by the payment of page charges. Therefore, and solely to indicate this

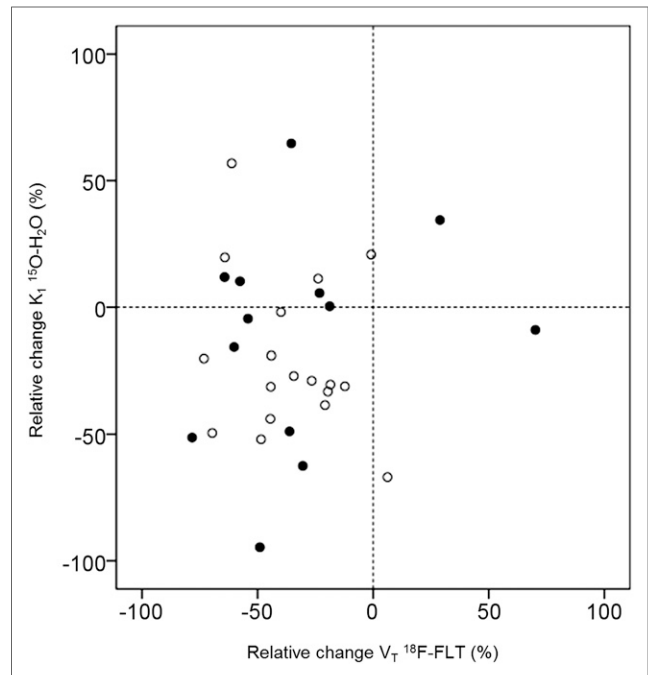


FIGURE 4. Correlation of percentage change in perfusion and proliferation, measured as K_1 of ^{15}O - H_2O and V_T of ^{18}F -FLT at 7 d (○) and 28 d (●) after start of treatment.

fact, this article is hereby marked “advertisement” in accordance with 18 USC section 1734. The research leading to these results has received support from the Innovative Medicines Initiative Joint Undertaking (www.imi.europa.eu; grant agreement number 115151), whose resources are composed of a financial contribution from the European Union’s Seventh Framework Programme (FP7/2007-2013) and an in-kind contribution from the companies of the European Federation of Pharmaceutical Industries and Associations. No other potential conflict of interest relevant to this article was reported.

ACKNOWLEDGMENTS

We thank the patients and their families for participating in this study. We also thank Arifa Moons-Pasic, Saskia Oedjaghir, Arthur Smit, Tineke Lammers, Martin Bard, Alle Welling, Roland Stallaert, and Roald Roeleveld for their help with patient recruitment for this study. In addition, we acknowledge the staff of the Department of Radiology and Nuclear Medicine of the VU University Medical Center, Amsterdam, The Netherlands, for their help with tracer production and data collection. The authors are members of the QuIC-ConCePT Consortium, whose participants include AstraZeneca, the European Organisation for Research and Treatment of Cancer (EORTC), Cancer Research U.K., the University of Manchester, Westfälische Wilhelms-Universität Münster, Radboud University Nijmegen Medical Center, Institut National de la Santé et de la Recherche Médical, Stichting Maastricht Radiation Oncology “Maastricht Clinic,” VUmc Amsterdam, King’s College London, Universitair Ziekenhuis Antwerpen, Institute of Cancer Research–Royal Cancer Hospital, Erasmus Universitair Medisch Centrum Rotterdam, Imperial College of Science Technology and Medicine, Keosys S.A.S., Eidgenössische Technische Hochschule Zürich, Amgen NV, Eli Lilly and Company Ltd., GlaxoSmithKline Research & Development Limited,

REFERENCES

1. D'Addario G, Fruh M, Reck M, Baumann P, Klepetko W, Felip E. Metastatic non-small-cell lung cancer: ESMO Clinical Practice Guidelines for diagnosis, treatment and follow-up. *Ann Oncol*. 2010;21(suppl 5):v116–v119.
2. Rami-Porta R, Crowley JJ, Goldstraw P. The revised TNM staging system for lung cancer. *Ann Thorac Cardiovasc Surg*. 2009;15:4–9.
3. Pikor LA, Ramnarine VR, Lam S, Lam WL. Genetic alterations defining NSCLC subtypes and their therapeutic implications. *Lung Cancer*. 2013;82:179–189.
4. Kobayashi T, Koizumi T, Agatsuma T, et al. A phase II trial of erlotinib in patients with EGFR wild-type advanced non-small-cell lung cancer. *Cancer Chemother Pharmacol*. 2012;69:1241–1246.
5. Rosell R, Carcereny E, Gervais R, et al. Erlotinib versus standard chemotherapy as first-line treatment for European patients with advanced EGFR mutation-positive non-small-cell lung cancer (EORTAC): a multicentre, open-label, randomised phase 3 trial. *Lancet Oncol*. 2012;13:239–246.
6. Mok TS, Wu YL, Thongprasert S, et al. Gefitinib or carboplatin-paclitaxel in pulmonary adenocarcinoma. *N Engl J Med*. 2009;361:947–957.
7. Thongprasert S, Duffield E, Saijo N, et al. Health-related quality-of-life in a randomized phase III first-line study of gefitinib versus carboplatin/paclitaxel in clinically selected patients from Asia with advanced NSCLC (IPASS). *J Thorac Oncol*. 2011;6:1872–1880.
8. Tan DS, Thomas GV, Garrett MD, et al. Biomarker-driven early clinical trials in oncology: a paradigm shift in drug development. *Cancer J*. 2009;15:406–420.
9. Chalkidou A, Landau DB, Odell EW, Cornelius VR, O'Doherty MJ, Marsden PK. Correlation between Ki-67 immunohistochemistry and ¹⁸F-fluorothymidine uptake in patients with cancer: a systematic review and meta-analysis. *Eur J Cancer*. 2012;48:3499–3513.
10. Sohn HJ, Yang YJ, Ryu JS, et al. [¹⁸F]fluorothymidine positron emission tomography before and 7 days after gefitinib treatment predicts response in patients with advanced adenocarcinoma of the lung. *Clin Cancer Res*. 2008;14:7423–7429.
11. Frings V, de Langen AJ, Yaqub M, et al. Methodological considerations in quantification of 3'-deoxy-3'-[¹⁸F]fluorothymidine uptake measured with positron emission tomography in patients with non-small cell lung cancer. *Mol Imaging Biol*. 2014;16:136–145.
12. Frings V, van der Veldt AAM, Boellaard R, et al. Pemetrexed induced thymidylate synthase inhibition in non-small cell lung cancer patients: a pilot study with 3'-deoxy-3'-[¹⁸F]fluorothymidine positron emission tomography. *PLoS ONE*. 2013;8:e63705.
13. Wieder HA, Geinitz H, Rosenberg R, et al. PET imaging with [¹⁸F]3'-deoxy-3'-fluorothymidine for prediction of response to neoadjuvant treatment in patients with rectal cancer. *Eur J Nucl Med Mol Imaging*. 2007;34:878–883.
14. Zander T, Scheffler M, Nogova L, et al. Early prediction of nonprogression in advanced non-small-cell lung cancer treated with erlotinib by using [¹⁸F]fluoro-deoxyglucose and [¹⁸F]fluorothymidine positron emission tomography. *J Clin Oncol*. 2011;29:1701–1708.
15. Gunn RN, Gunn SR, Cunningham VJ. Positron emission tomography compartmental models. *J Cereb Blood Flow Metab*. 2001;21:635–652.
16. Lubberink M, Direcks W, Emmering J, et al. Validity of simplified 3'-deoxy-3'-[¹⁸F]fluorothymidine uptake measures for monitoring response to chemotherapy in locally advanced breast cancer. *Mol Imaging Biol*. 2012;14:777–782.
17. Surti S, Kuhn A, Werner ME, Perkins AE, Kolthammer J, Karp JS. Performance of Philips Gemini TF PET/CT scanner with special consideration for its time-of-flight imaging capabilities. *J Nucl Med*. 2007;48:471–480.
18. Machulla HJ, Blocher A, Kuntzsch M, Piert M, Wei R, Grierson JR. Simplified labeling approach for synthesizing 3'-deoxy-3'-[¹⁸F]fluorothymidine ([¹⁸F]FLT). *J Radioanal Nucl Chem*. 2000;243:843–846.
19. de Langen AJ, Klabbbers B, Lubberink M, et al. Reproducibility of quantitative ¹⁸F-3'-deoxy-3'-fluorothymidine measurements using positron emission tomography. *Eur J Nucl Med Mol Imaging*. 2009;36:389–395.
20. Vanderhoeck M, Perlman SB, Jeraj R. Impact of the definition of peak standardized uptake value on quantification of treatment response. *J Nucl Med*. 2012;53:4–11.
21. Frings V, Schouten R, Velasquez LM, et al. Repeatability of metabolically active tumor volume of [¹⁸F]FDG PET-CT in a multicenter setting [abstract]. *J Nucl Med*. 2013;54(suppl 2):4P.
22. van der Veldt AAM, Hendrikse NH, Harms HJ, et al. Quantitative parametric perfusion images using ¹⁵O-labeled water and a clinical PET/CT scanner: test-retest variability in lung cancer. *J Nucl Med*. 2010;51:1684–1690.
23. Yaqub M, Boellaard R, Kroppholler MA, Lammertsma AA. Optimization algorithms and weighting factors for analysis of dynamic PET studies. *Phys Med Biol*. 2006;51:4217–4232.
24. Tomasi G, Kimberley S, Rosso L, Aboagye E, Turkheimer F. Double-input compartmental modeling and spectral analysis for the quantification of positron emission tomography data in oncology. *Phys Med Biol*. 2012;57:1889–1906.
25. Sugawara Y, Zasadny KR, Neuhoff AW, Wahl RL. Reevaluation of the standardized uptake value for FDG: variations with body weight and methods for correction. *Radiology*. 1999;213:521–525.
26. Akaike H. A new look at the statistical model identification. *IEEE Trans Automat Contr*. 1974;19:716–723.
27. Contractor KB, Kenny LM, Coombes CR, Turkheimer FE, Aboagye EO, Rosso L. Evaluation of limited blood sampling population input approaches for kinetic quantification of [¹⁸F]fluorothymidine PET data. *EJNMMI Res*. 2012;2:11.
28. Muzi M, Vesselle H, Grierson JR, et al. Kinetic analysis of 3'-deoxy-3'-fluorothymidine PET studies: validation studies in patients with lung cancer. *J Nucl Med*. 2005;46:274–282.
29. Perumal M, Pillai RG, Barthel H, et al. Redistribution of nucleoside transporters to the cell membrane provides a novel approach for imaging thymidylate synthase inhibition by positron emission tomography. *Cancer Res*. 2006;66:8558–8564.
30. Kenny LM, Contractor KB, Stebbing J, et al. Altered tissue 3'-deoxy-3'-[¹⁸F]fluorothymidine pharmacokinetics in human breast cancer following capecitabine treatment detected by positron emission tomography. *Clin Cancer Res*. 2009;15:6649–6657.
31. Wahl RL, Jacene H, Kasamon Y, Lodge MA. From RECIST to PERCIST: evolving considerations for PET response criteria in solid tumors. *J Nucl Med*. 2009;50(suppl 1):122S–150S.
32. Galvani E, Alfieri R, Giovannetti E, et al. Epidermal growth factor receptor tyrosine kinase inhibitors: current status and future perspectives in the development of novel irreversible inhibitors for the treatment of mutant non-small cell lung cancer. *Curr Pharm Des*. 2013;19:818–832.
33. Wu JY, Wu SG, Yang CH, et al. Comparison of gefitinib and erlotinib in advanced NSCLC and the effect of EGFR mutations. *Lung Cancer*. 2011;72:205–212.
34. Cheebsumon P, Velasquez LM, Hoekstra CJ, et al. Measuring response to therapy using FDG PET: semi-quantitative and full kinetic analysis. *Eur J Nucl Med Mol Imaging*. 2011;38:832–842.